International Microelectronics Assembly and Packaging Society
Bringing together the entire microelectronics supply chain™

Solutions for thermally mismatched brazing operations for ceramic tokamak magnetic sensor

Caroline Jacq, Thomas Maeder, Benoit R. Ellenrieder, Philipp Windischhofer, Xinyue Jiang, Matthieu Toussaint, Duccio Testa, Peter Ryser
EPFL - École Polytechnique Fédérale de Lausanne, Switzerland
EPFL-IMT-LPM, BM0.141, station 17
CH-1015 Lausanne
+41.24.693.53.85, FAX +41.21.693. 38.91
caroline.jacq@epfl.ch

Abstract

To monitor high-frequency fluctuations of the equilibrium magnetic field in tokamaks, a 3D magnetic sensor has been developed. The sensor, which is positioned inside the vacuum vessel behind the protective tiles of the tokamak and is exposed to potential temperatures up to 400°C, is based on thick-film and LTCC (low-temperature co-fired ceramic) technology. To connect the sensor to the cabling that runs inside the vacuum vessel, mineral-insulated cables have to be brazed to the sensor to ensure electrical connection together with mechanical robustness and sufficient thermal stability. As the brazing temperature is about 600°C, direct brazing to the alumina sensor substrate can cause failure by cracking induced by thermal stresses. It arises both by temperature gradients stemming from the localised heating and by the high thermal mismatch of alumina with the braze and wire materials. In previous work, high stresses from temperature gradients were efficiently decoupled by brazing indirectly to alumina beams attached to the main substrate, and local thermal stresses between alumina and braze/wire by using a porous metallisation. However, as the slender alumina beams protruding out of the substrate are somewhat cumbersome and fragile, three alternatives were studied in the present work: 1) testing shorter and more robust beams, 2) replacing the alumina beam by a silver wire, and 3) depositing a porous temperature- and stress-decoupling dielectric to enable direct brazing on the main alumina substrate. These solutions are characterised with respect to their mechanical robustness and of the degree of thermal decoupling with the substrate they provide.

Keywords: Stress decoupling, thick-film technology, porous metallisation.

Introduction

Plasma confinement in tokamak fusion devices such as the ITER is ensured by applying toroidal and poloidal magnetic fields inside the chamber. These large magnetic fields need to be adjusted in real time [1], to compensate fluctuations such as MHD (magnetohydrodynamic) instabilities in the plasma, which requires appropriate sensors capable of operation under neutron flux and at temperatures up to ~300°C. To this end, a 3D magnetic field sensor (Figure 1), based on thick-film and LTCC (low-temperature cofired ceramic) technology, has been developed [2,3] and optimised to achieve sufficient signal and bandwidth in every direction [4] to the frequency range from 5 kHz to 1 MHz.

For integration within the walls of the tokamak, the sensor has to be connected to the mineral-insulated cabling, which is carried out by brazing to ensure sufficient thermal stability.

As the brazing temperature is about 600°C, direct brazing to the alumina sensor substrate can cause failure by cracking induced by thermal stresses. It is due to both by temperature gradients from the localised heating and the high thermal mismatch of alumina with the braze and wire materials. In previous work [5], high stresses from temperature gradients were efficiently decoupled by brazing indirectly to alumina beams attached to the main substrate covered with porous silver metallisation to decouple the local thermal stresses between alumina and braze/wire. The beams are sealed to the sensor base and have to perfectly suit to a MACOR ceramic support depicted on the Figure 2. This solution responses with satisfaction for the thermal decoupling. However, as the slender alumina beams (25 mm length) protruding out of the substrate are somewhat cumbersome and fragile, especially during the positioning in the glass-ceramic (MACOR©, machinable fluor-phlogopite composition [5]) ceramic support (Figure 2), where the beams have to be perfectly aligned to the glass-ceramic support.

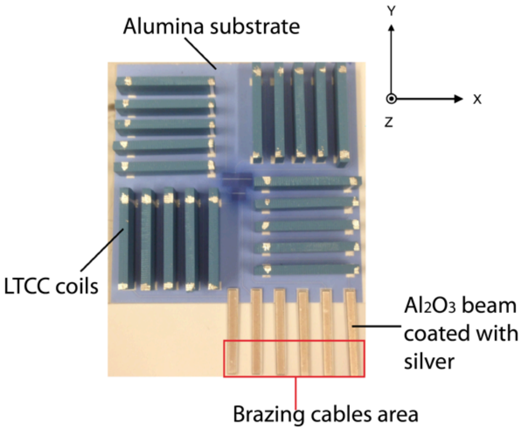

Figure 1: 3D magnetic sensor for high frequency measurement

In this work, in order to make the sensor more compact, improve the robustness of the connection sensor-cable without degrading the thermal decoupling towards the braze face to the sensor, three solutions were investigated.

1. Simply shortening the alumina beams
2. Replacing the alumina beams by silver wire
3. Replacing alumina beam with a porous dielectric

Each solution has been characterised with respect to its ease of fabrication, robustness, the size of the sensor and the thermal decoupling, which have been evaluated by calculation of the thermal resistance for the three solutions. A final test has then been carried out, where the three solutions have been brazed, to assess the thermal stress with the alumina substrate.

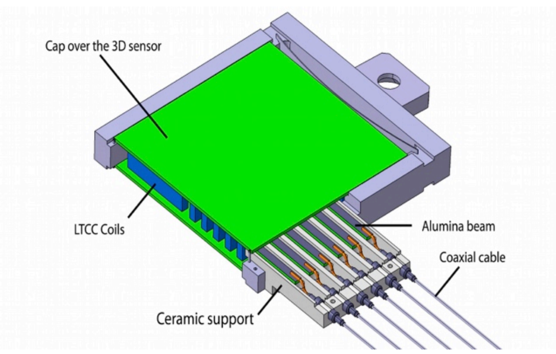

Figure 2: 3D magnetic sensor placed in the support for the in-vessel installation

Experimental

Shorter alumina beams

The aim of using shorter alumina beams is to improve the mechanical resistance in flexion and thus reduce the risk of breakage. The beams are 96% thick-film grade (A-476, Kyocera, Japan) alumina substrate rectangles, 12.5 mm long, 3 mm wide and 0.8 mm thick. The sensor is then somewhat also more compact, as the MACOR ceramic support is correspondingly smaller.

For the characterisation of thermal decoupling, the alumina beams have not been covered with silver layers. The beams have been covered with silver only for the final brazing tests. The beams are sealed to similar alumina base substrate (1 mm thick) with silver pads. The paste is the same paste used in previous study [6], a mixture of low-firing Ag composition ESL (ElectroScience Laboratories, USA) 590G and "V6" glass [7], yielding an estimated 37% glass and 63% Ag by volume, fired in a belt furnace at a peak temperature of 600°C, with 10 min peak dwell time (45 min total).

To characterise the thermal decoupling, an SMD high power chip resistor (47 Ω, 3W) heating source has been used to simulate the heating due to the braze (albeit at a lower temperature). This heating resistor is fixed to the extremity of the beam with a thermally conducting silicone glue (Q5-8401, Dow Corning, USA, filled with 30% vol. Al_2O_3 ~10 µm powder). Pt-1000 resistors are then attached with Dow Corning 340 heat sink compound at different places along the beam and the substrate to measure the temperature (Figure 3).

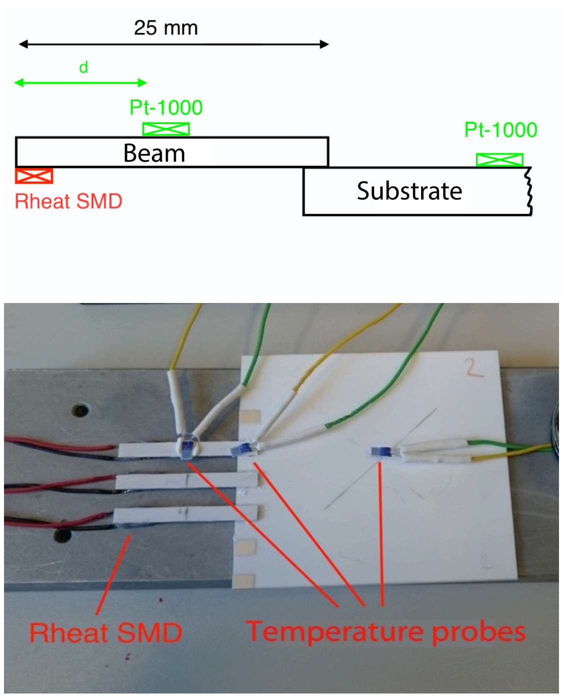

Figure 3: Measuring setup for the shorter beams solution

Silver wire

For the second solution, the beam is replaced by a silver wire. The soft, malleable silver wire suits perfectly the MACOR ceramic support. Silver wires, Ø 0.37 mm (Advent Research, 99.99%), 5 cm length, have been sealed with a paste of the aforementioned mixture (ESL 590G + V6 glass) using the same 600°C 10 min profile to an alumina substrate (50×50 mm^2, 1 mm thick).

To thermally characterise this solution, some SMD 47 Ω, 3W resistors are soldered along the silver wire as a heat source. The temperature is measured with Pt-1000 resistors mounted on pad soldered along the silver wire. The setup is depicted on Figure 4.

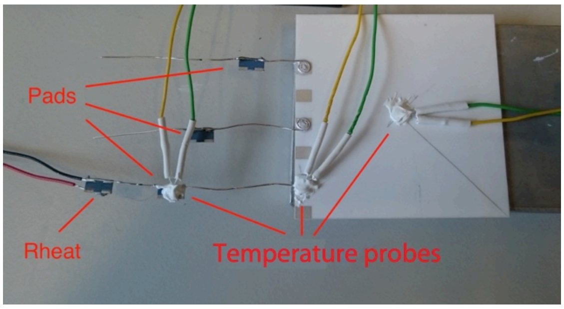

Figure 4: Test setup for the silver tracks solution

Porous dielectric

The aim of this solution is to make the sensor even more compact, as the braze is directly on the substrate and the thermal decoupling is vertical instead of horizontal for both other solutions. This vertical structure is composed of successively-deposited layers on the alumina substrate, as depicted on Figure 5. The first dense dielectric layer ensures good adhesion on the substrate. Then, a thick porous dielectric layer (~140-530 µm) is screen-printed for the thermal decoupling. A dense dielectric layer is again deposited to ensure sound deposition of the following sandwich dense/porous/dense silver layer, with the porous layer decreasing the stresses [6] induced by the difference of thermal coefficient of expansion between the braze and the dielectric during the cooling.

Four porous dielectric compositions (Table 1) have been formulated, based on two commercial dielectric pastes ESL 4913 (more crystalline) and ESL 4917 (more glassy), mixed together and with graphite powder (KS5-44, 5-44 µm, TIMCAL, Switzerland).

To evaluate these variants of the porous dielectric solution, the samples have been manufactured according to the layout depicted on Figure 6 on 50×50 mm^2 1 mm thick alumina substrate. Two positive temperature coefficient (PTC) resistors (one resistor to heat and the other to measure the heat, ESL 2611-I-Special) have been screen-printed onto a sandwich of dense/porous/dense dielectric with Ag terminations / tracks. All layers were fired at 850°C (dwell 10 min, total 45 min), with multiple firings necessary for thick porous dielectric layers.

For the thermal characterisation, the sample was placed with Dow Corning 340 compound onto an aluminium plate to ensure a good thermal connection. The temperature of the Al plate close to the substrate was monitored with a Pt-1000 resistor, as depicted on Figure 7.

Table 1. Porous dielectric compositions

	4913 : 4917 weight ratio	KS5-44 (% vol. vs dielectric)
000Pb	1:0	50
033Pb	2:1	50
067Pb	1:2	50
100Pb	0:1	50

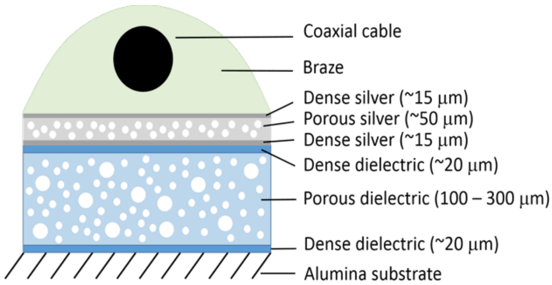

Figure 5: Schema of the porous dielectric/silver solution

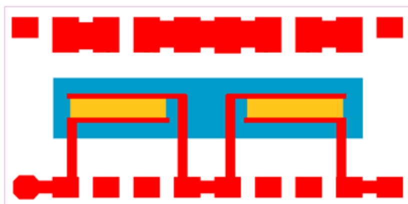

Figure 6: Layout of porous dielectric sample

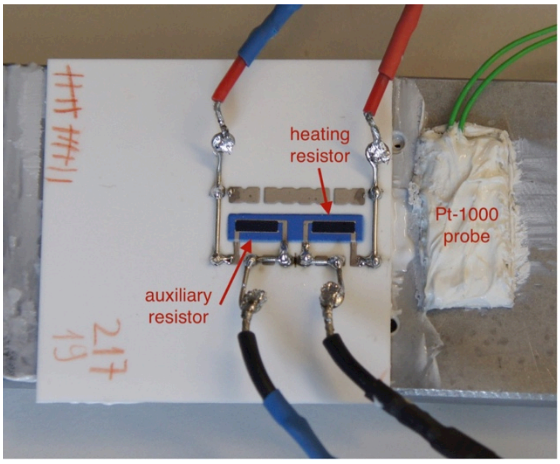

Figure 7: Porous dielectric setup

Neglecting convective and radiative losses, the heat induced by developing a power P by the heating resistor, yielding a temperature T_{heat}, diffuses to the alumina substrate (temperature T_{subs}) through the porous dielectric, whose thermal resistance R_{th} may be calculated according the equation (1):

$$R_{th} = \frac{T_{heat} - T_{subs}}{P} \quad \textbf{(1)}$$

Given that the temperature of the substrate immediately below the dielectric is not directly measurable, the thermal resistance has been calculated by incrementation between successive measurements on a short time frame, allowing to consider T_{subs} to remain constant due to the higher thermal capacity of the alumina substrate compared to the porous dielectric.

Results and discussion

Porous dielectric

All the measurements are evaluated considering only conduction through the dielectric and neglecting both convection and radiation. The thermal resistance of the dielectric, represented in the Figure 8, for four porous dielectric compositions increases linearly with the thickness of the dense and porous dielectric layers. Presumably due to its higher glass content (more sintering), the 100Pb composition has a somewhat lower thermal resistance. Further sintering of this more glassy composition is also postulated to be the cause of the breakdown of the linear increase of thermal resistance with thickness observed for very thick layers (~500 µm), due to the multiple firings needed to build up those layers.

The thermal conductivity of the other compositions (000Pb, 033Pb and 067Pb), determined from these results, is essentially constant and lies in the 0.5-0.6 W/m/K range.

Shear tests have been also been carried out on the samples to evaluate the robustness of the porous dielectric layer. To this end, screws have been soldered (Sn62 solder, 62% Sn + 36% Pb + 2% Ag by weight) to an upper dense silver layer screen-printed onto the sandwich of dielectrics (Figure 9).

As a reference, the test was first carried out without the porous silver layer, yielding a rupture shear stress of (10.2 ± 2.6) MPa. Rupture occurs at the interface between the Ag pad and the dielectric and in the porous dielectric.

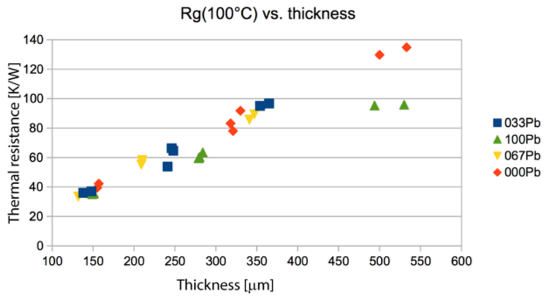

Figure 8: Thermal resistance R_{th} vs porous dielectric thicknesses for the 4 dielectric compositions

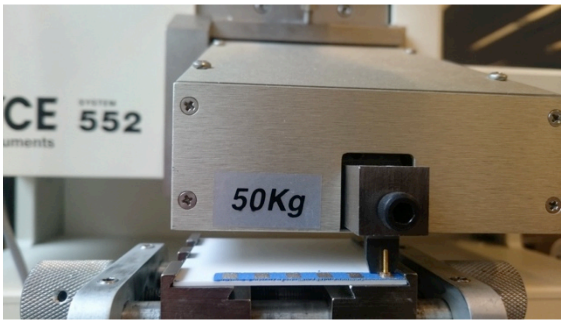

Figure 9: Shear test

Shorter beam

The heating power P is calculated from equation (2), where λ is the thermal conductivity of the beam, A its cross section, d the distance between measuring points, and T_H and T_L the temperature of the measuring points (measured at 12.5 and 25 mm from the heating source, for T_H and T_L respectively):

$$P = \lambda \cdot \frac{A}{d} \cdot (T_H - T_L) \quad \textbf{(2)}$$

Figure 10 represents the temperature variation along the beam from the heating resistor to the substrate at three power levels. The thermal resistance has been calculated for 3 relatively low temperatures in a narrow range, in order to avoid significant convective and radiative losses around the SMD heating resistor, choosing the thermal conductivity for Al_2O_3-96% to 20 W/m/K [8]. The results are reported in Table 2.

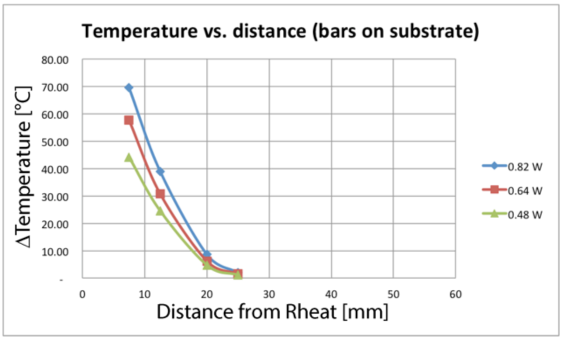

Figure 10: Temperature variation with the room temperature measured at different power along the beam from the heat resistor

Table 2: Thermal resistance at 3 power levels

Temperature (°C)	Power (W)	Thermal resistance (K/W)
50	0.48	297
55	0.64	296
65	0.84	299

Silver wire

The temperature increase at different positions along the ~50 mm long Ag wire is depicted as a function of applied heating power P_{In} in Figure 11. Regarding this variant, despite the high thermal conductivity of silver, the temperature increase is found to decay strongly with distance from the heating source, with only little heating observed at 39 mm from the heating source.

From the temperature profile, it is found that only part of the heating power is eventually transmitted to the substrate, with this fraction being only ca. one quarter at 39 mm from the source, and somewhat decreasing with increasing heating power. This leads us to postulate losses by natural convection along the wire, which was confirmed by both calculations [9], and measurements on long Ag wires not attached to the substrate, where temperature also drops with distance from the heating source, despite the absence of a solid heat sink.

The observed somewhat faster decay of temperature along the wire at higher powers agrees with the corresponding increase of the dissipation coefficient due to natural convection at higher temperature [9], combined with the decrease of the thermal conductivity of silver [10]. The corresponding calculated critical length (where convective losses become larger than conduction along the wire) is ~25 mm, and estimated [9,10] to drop to ~20 mm at 500°C. This effect favourably decreases thermal stresses in the substrate.

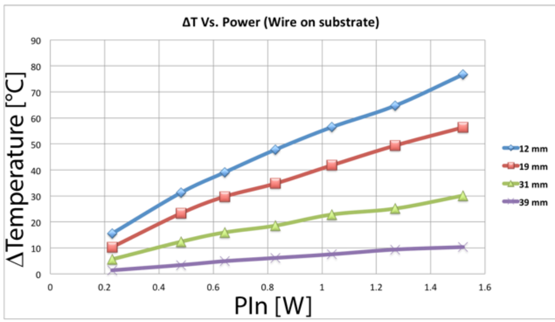

Figure 11: Temperature variation vs ambient ΔTemperature vs resistor heating power P_{In}, measured along the wire at different distances from the heating resistor (~50 mm total length).

Brazing test for the three solutions

Coaxial cables have been brazed at ~600°C with the silver braze Castolin 1802F, for the three solutions as depicted on Figure 12. The brazing operation has been carried out with the substrate placed on a hotplate (81-90°C, Table 3) to somewhat reduce the temperature difference and thereby the thermal stress in the alumina substrate. The resulting assemblies are shown in Figure 13.

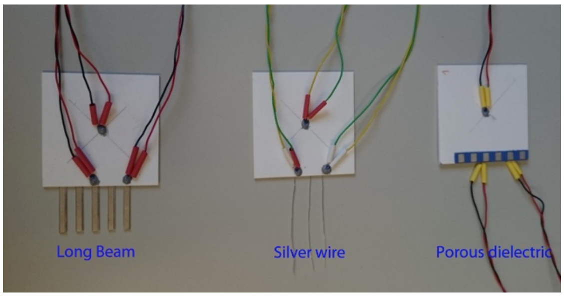

Figure 12: Test samples with alumina beam, silver wire and porous dielectric as connection support for brazing

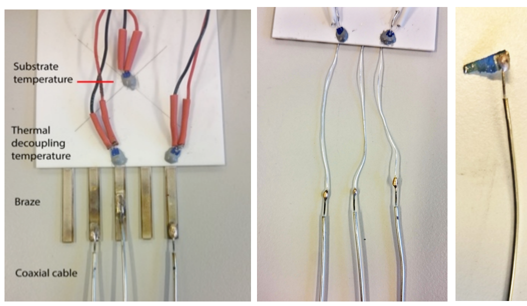

Figure 13: Coaxial cables brazed on beam, silver wire and porous dielectric supports (from left to right)

The maximal temperatures are measured on the substrate (~25 mm from the edge, T_{subs}) and near the edge of the substrate, at the junction to the thermal decoupling structure (T_{TD}) for each case, and are reported in Table 3, together with the reference thermal stress σ_{th}:

$$\sigma_{th} = \alpha \cdot E \cdot (T_{TD} - T_{subs}) \quad \textbf{(2)}$$

Here, α is the thermal expansion coefficient and E the Young's modulus of alumina. It must be emphasised that this is a reference stress only; this stress is estimated to largely translate into an (uncritical) compressive stress near the edge, with the actual critical stress (maximum tensile one) being much lower.

The calculated value of σ_{th} is much lower for the long beam and silver wire cases (the small differences of hotplate temperature play a negligible role). The shorter beams and especially the porous dielectric yield higher, but still presumably uncritical substrate stresses. However, the critical stresses for the latter solution occur within the porous dielectric, and lead to damage: the dielectric breaks very easily with a low finger pressure on the soldering pad. Also, this solution is not as practical as expected for manual brazing: it is more difficult to observe the brazing operation due to the flame being reflected by the substrate, and the metallisation is found to leach quickly due to the low heated mass.

Table 3: Thermal decoupling results

	Long beam	Short beam	Silver wire	Porous dielectric
Tmax thermal decoupling (°C)	97	139	98	179
Substrate Tmax (°C)	85	94	94	92
Heating plate Temperature (°C)	81	90	90	89
Thermal stress (Mpa)	31	111	10	204

Conclusion

As the conclusion, to connect the 3D magnetic sensor with braze and suitable materials for nuclear fusion environment, three solutions (short alumina beams, Ag wire and porous dielectric) have been examined to thermally decouple the sensor substrate from the brazing area, considering also the robustness of the assembly and ease of operation. Shorts beams, which are more robust than long beams, present lower thermal decoupling performance, but this remains acceptable, making this solution a possible one. Porous dielectric is the most compact solution, but presents the lowest degree of thermal decoupling. Although this decoupling remains acceptable for the alumina substrate, the porous dielectric does not withstand the very high thermal gradient across it, and undergoes damage during brazing. Finally, the best solution is the silver wire, which is soft and malleable, easily brazed and furthermore ensures the highest degree of thermal decoupling. Further studies will concentrate on the attachment of the silver wire, which still requires some improvement.

References

[1] D. Testa, R. Chavan, J. Guterl, J.B. Lister, J.M. Moret, A. Perez, F. Sanchez, B. Schaller, G. Tonetti, M. Toussaint, G. Chitarin, R.S. Delogu, A. Gallo, N. Marconato, S. Peruzzo, H. Carfantan, A. Encheva, G. Vayakis, C. Walker, E. Hodgson, J. Romero, R. Vila, Y. Fournier, T. Maeder, B. Brichard, L. Vermeeren, A. Le Luyer, P. Moreau, "The magnetic diagnostic set for ITER", IEEE Transactions on Plasma Science Vol. 38 (3), 284-294, 2010.

[2] M. Toussaint, D. Testa, N. Baluc, R. Chavan, Y. Fournier, J.B. Lister, T. Maeder, P. Marmillod, F. Sanchez & M. Stöck, "Design of the ITER high-frequency magnetic diagnostic coils", poster, 26th Symposium on Fusion Technology, Porto (PT), 2010.

[3] D. Testa, Y. Fournier, T. Maeder, M. Toussaint, R. Chavan, J. Guterl, J.B. Lister, J.M. Moret, B. Schaller, G. Tonetti, "Prototyping a high frequency inductive magnetic sensor using the nonconventional, low temperature co-fired ceramic technology for use in ITER", Fusion Science and Technology Vol. 59 (2), 376-396, 2011.

[4] D. Testa, A. Corne, G. Farine, C. Jacq, T. Maeder, M. Toussaint, "3D, LTCC-type, high-frequency magnetic sensors for the TCV Tokamak", Fusion Engineering and Design Vol. 96-97, 989-992, 2015.

[5] Z. Strnad, "Glass-Ceramic Materials", Glass Science and Technology, Elsevier, Amsterdam (NL) 8, 1986.

[6] C. Jacq, T. Maeder, L. Güniat, A. Corne, D. Testa, P. Ryser, "Porous thick-film metallisation for thermally mismatched brazing operations in tokamak magnetic sensor", Proceedings, 11th International CICMT conference and Exhibition of IMAPS/ACerS, Dresden, Germany, 2015.

[7] S. Vionnet Menot. "Low firing temperature thick-film piezoresistive composites – properties and conduction mechanism, thesis n°3290 (2005).

[8] J. Kita, F. Schubert, F. Rettig, A. Engelbrecht, A. Groß, R. Moos, "Ceramic alumina substrates for high-temperature gas sensors – Implications for applicability", Proceedings, the XXVIII edition of the conference series of Eurosensors 2014, Brescia, Italy, 2014.

[9] S. Boetscher, "Natural convection heat transfer from horizontal cylinders", SpringerBriefs in Thermal Engineering and Applied Science, ISBN 978-3-319-08132-8, chapter 2, 3-22, 2014.

[10] R.W. Powell, C.Y Ho, P.E. Liley, "Thermal conductivity of selected materials", NSRDS-NBS 8 - National Standards Reference Data Series, National Bureau of Standards (USA), 1966.